Bio-Inspired Superoleophobic Fluorinated Wax Crystalline Surfaces

*Sasha Pechook, Noga Kornblum, and Boaz Pokroy**

A novel, single-step and single-component bio-inspired fabrication method of hierarchical superoleophobic surfaces is presented. The method consists in thermal deposition of self-assembling ultra-low-surface-energy fluorinated wax on diverse surfaces. The thermal deposition results in crystalline, oriented, three-dimensional hierarchical structures with high surface roughness and re-entrant curvature, which in combination with the low surface energy of the fluorinated wax results in high contact angles of low-surface-tension liquids and low contact-angle hysteresis (CAH) values ($\Delta\theta$). The values achieved for $\Delta\theta$ are below 10° even for ethanol, which exhibits a surface tension as low as 22.4 mN·m^{-1}. In addition to their superoleophobic properties our substrates exhibit extreme superhydrophobic qualities (CAH as low as 2° and contact angle >170°) with exceptional surface stability over many months. The proposed fabrication method may be utilized for a variety of applications where non-wetting of low-surface-tension liquids is required, for example non-staining surfaces and antifouling. The ease of fabrication and the variety of substrates that can be modified will undoubtedly widen its use.

1. Introduction

Superhydrophobicity has been widely studied and utilized in numerous applications in recent years. These applications range from drag reduction[1] through antifouling[2] to self-cleaning surfaces[3] and anti-icing.[4] The inspiration for this effect was found in nature in a variety of insects such as butterfly wings and water striders,[5] and in various plants[6] of which the lotus leaf is the best-known example.[7] On such surfaces, water displays contact angles that exceed 150° and contact angle hysteresis (CAH) lower than 10°. There are two main contributors to the superhydrophobic phenomenon: the surface chemistry (i.e., surface energy) and the surface roughness, both of which have been thoroughly investigated.[8] While Young's equation[9] gives the equilibrium contact angle (θ_0) on a smooth surface as a function of the interfacial tensions, the models of Wenzel (homogeneous surfaces)[10] and Cassie–Baxter (heterogeneous surfaces)[11] provide the roughness contribution to the wettability (θ^*). The formation and stability of a superhydrophobic state depend on several factors, including droplet curvature, Young's contact angle, and local inhomogeneities.[8b,f,g,12]

The requirement for $\theta_0 > 90°$ in order to achieve $\theta^* > 150°$ is a barrier to the fabrication of superoleophobic surfaces. These surfaces, however, form an apparent contact angle of $\theta^* > 150°$ with any liquid, including low-surface-tension liquids such as ethylene-glycol ($\sigma = \gamma_{lv} = 47.4$ mN·m^{-1}) and ethanol ($\sigma = \gamma_{lv} = 22.4$ mN·m^{-1}).[13] To form an intrinsic contact angle of $\theta_0 = 90°$ with a low-surface-tension liquid (γ_{lv}), the substrate surface energy (γ_{sv}) must be equal to the solid/liquid surface tension (γ_{sl}).[14] Whereas a considerable body of literature is devoted to superhydrophobic natural and artificial substrates, there are significantly fewer published reports of superoleophobic (i.e., low-surface-energy) surfaces.

Several studies have shown extremely high water-contact angles on surfaces with $\theta_0 < 90°$,[8d,15] owing to the formation of metastable Cassie states.[16] This can also be implemented for the formation of metastable superoleophobic surfaces. Other methods for the formation of superoleophobic surfaces have been suggested, most of which are intricate and combine the formation of surface roughness and surface treatment with a low-surface-energy compound, chosen mainly from fluorinated compounds, known for their low surface energy.[17] Among the suggested methods are spin-coating of a polymer blended with fluoroPOSS molecules,[18] fabrication of re-entrant curvature structures produced by SiO_2 deposition,[18] a sequential two-step etching process and surface treatment with perfluorodecyltrichlorosilane allowing the formation of $\theta^* >> 90°$ for the case of $\theta_0 < 90°$,[18] treatment of anodically oxidized aluminum with fluorinated compounds,[14] deposition of perfluoro-*n*-eicosane ($C_{20}F_{42}$) as a surface modifier on micro-patterned surfaces,[19] electrochemical polymerization of fluorinated polymers,[20] vapor-phase polymerization in the presence of fluorinated alkyls,[21] plasma treatments used for roughening and fluoroelement introduction,[22] formation of a rough and robust silica surface via a chemical vapor deposition procedure over a candle soot template,[23] formation of hierarchical structures with re-entrant curvature based on coatings of different micrometer-scaled mashes[13,24] and many others. Surfaces fabricated by McCarthy et al.[26] and the novel slippery surfaces suggested by Aizenberg et al.[25] are fabricated using a different approach

S. Pechook, N. Kornblum, Prof. B. Pokroy
Department of Materials Science & Engineering
and the Russell Berrie Nanotechnology Institute
Technion – Israel Institute of Technology
32000 Haifa, Israel
E-mail: bpokroy@tx.technion.ac.il

DOI: 10.1002/adfm.201203878

which is based on the practical definition of oleophobicity; the ability of the surface to resist droplet pinning. Such a surface might exhibit relatively low contact angles and a small CAH causing a droplet of liquid to move easily on such a surface, which would repel the liquid. Although conceptually very different, these methods as well as the structure-based methods require several production steps and at least two different components.

We present a novel single-step method for the fabrication of hierarchical superhydrophobic and superoleophobic substrates via thermal evaporation of $C_{24}F_{50}$-fluorinated wax based on our previous study with *n*-paraffin waxes.[27]

2. Results and Discussion

The method we used to fabricate substrates exhibiting superoleophobic properties was thermal evaporation of fluorinated wax. Our choice of this method was based on a previous study in our lab in which relatively high contact angles were demonstrated not only for water but also for glycerol (168°) and ethylene glycol (149°). In that study, hierarchical superhydrophobic surfaces were fabricated via thermal evaporation of *n*-paraffin waxes. In the present study, fluorinated wax ($C_{24}F_{50}$) was chosen because of the requirement for a low-surface-tension material[17b,19] and the relatively low melting temperature of the wax (Tm = 188 °C), allowing its thermal evaporation at low temperatures. Perfluorotetracosane layers, ≈1.0–1.5 µm thick, were thermally evaporated onto various substrates: a (1 0 0) silicon wafer, a glass slide, a (1 1 1) gold layer supported on Si and copper discs. After deposition, all samples were maintained at room temperature and characterized by the use of X-ray diffraction (XRD), confocal microscopy, high-resolution scanning electron microscopy (HR-SEM), and tensiometry.

2.1. Structure

The XRD measurements presented in **Figure 1** revealed the formation of crystalline layers on all examined substrates. In addition, similar preferred orientation was observed for the layers evaporated on Si, glass, and Au substrates. Based on the Joint Committee on Powder Diffraction Standards card for $C_{20}F_{42}$ (JCPDS #45-1589) and the assumption that perfluorotetracosane exhibits the same rhombohedral structure, we can state that the preferred orientation is of the (0 0 l) type. For this orientation, a majority of CF_3 groups is expected at the sample surface. The layers evaporated on Cu exhibited a preferred orientation, which is shown by the relatively prominent peak at 2θ~18° and is attributed to the (1 0 1) planes.

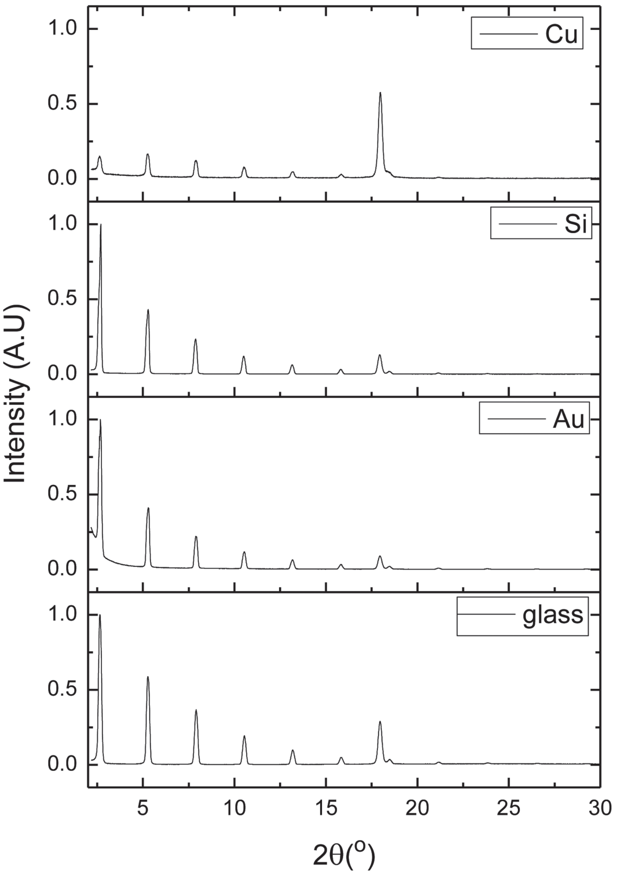

Figure 1. XRD spectrum of thermally deposited $C_{24}F_{50}$ films on copper, Si, gold, and glass substrates. Diffraction was carried out with Cu Kα.

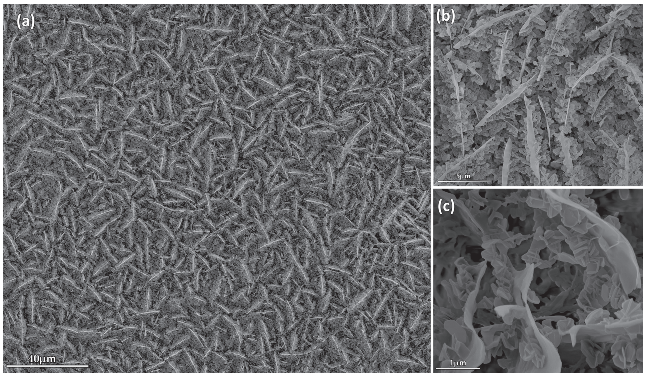

Figure 2. HR-SEM image showing the hierarchical structure of thermally deposited $C_{24}F_{50}$ on a Cu surface at different magnifications. a) ×1000, b) × 8000, and c) ×30 000.

HR-SEM measurements revealed an unexpected structure of the evaporated layer. The highly oriented platelets, observed at a magnification of ×1000 (**Figure 2**a), actually form a hierarchical structure composed of large, high platelets, ≈3–5 µm long and ≈1.2–3.0 µm high (height was measured by confocal microscopy, see **Figure 3**), oriented perpendicularly to the substrate at distances of 3.5–5.5 µm from one another, and a three-dimensional structure of significantly smaller platelets (≈300–500 nm long) deposited on top of the large platelets, parallel and perpendicularly to the substrate (Figure 2b). Higher magnification imaging (Figure 2c) revealed the combined structure of additional small platelets deposited perpendicularly on top of and perpendicular to the second level of platelets. A schematic illustration is presented in **Figure 4**a and the corresponding areas are marked in an HR-SEM image presented in Figure 4b. The structure exhibits extremely high surface roughness, as

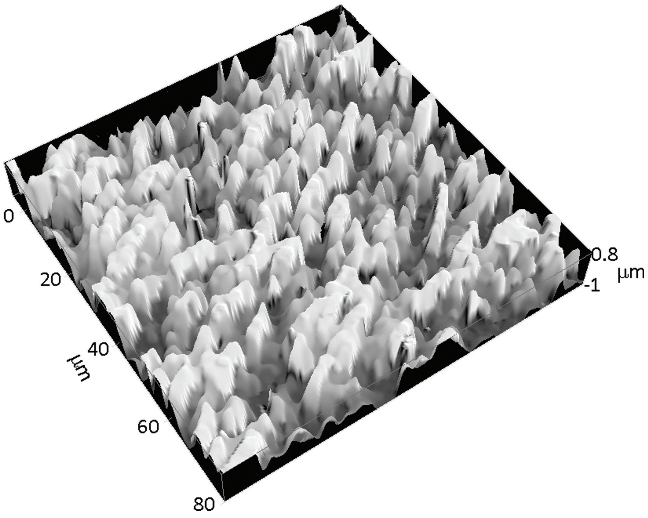

Figure 3. Confocal image showing the roughness of the wax-coated Si surface.

also indicated by the root mean square (RMS) roughness of 0.8–0.9 µm measured by confocal microscopy (Figure 3). Furthermore, the parallel and perpendicular crystals of this complex structure form re-entrant curvatures (Figure 4) that are well suited to the formation of superoleophobic surfaces.[18,28]

The main benefit of our fabrication method is the formation of a hierarchical structure during a single evaporation step with a single component (low-surface-energy fluorinated wax), compared to the sequential, two-component evaporation procedure required for the formation of similar structures using *n*-paraffin wax.

2.2. Contact-Angle Measurements

To examine the wettability properties of the substrates, we measured the static contact angles of liquids with different surface tensions (see **Table 1**) using a constant droplet volume of 7 µL, on the wax layers evaporated onto Si, glass, and Cu. To estimate the surface ability of Si, glass, and Cu substrates to

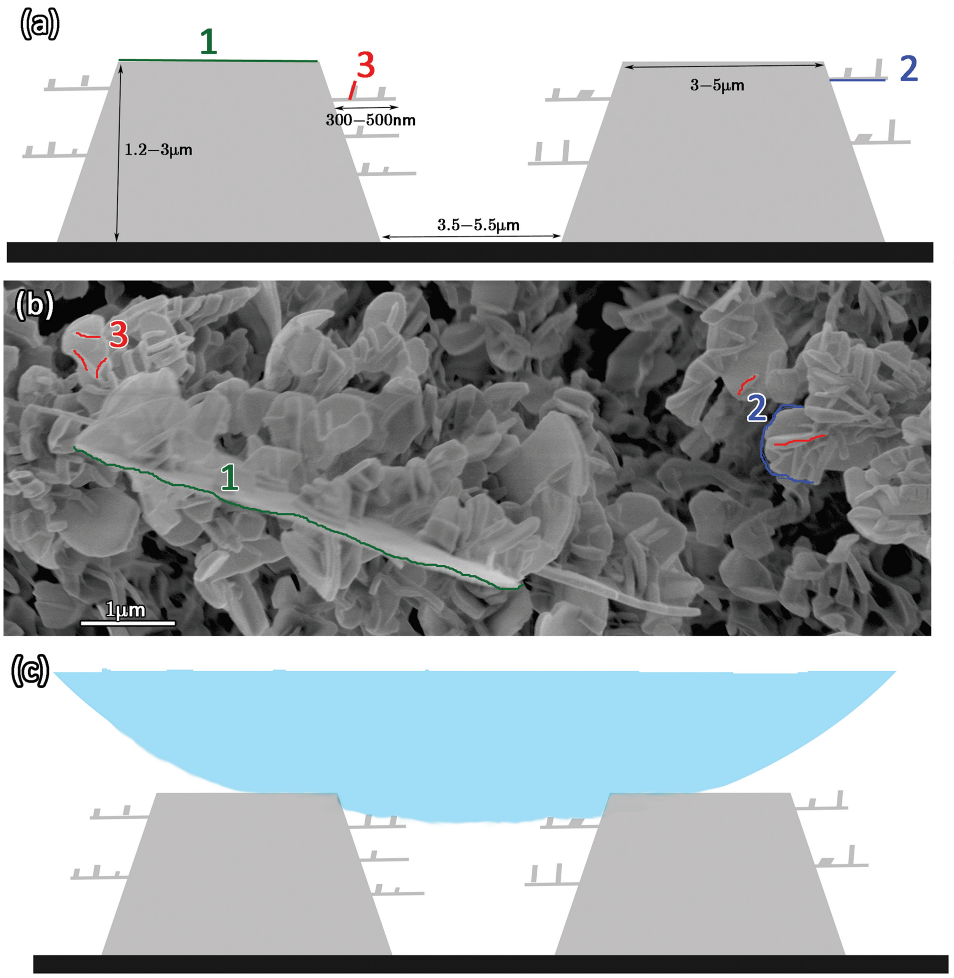

Figure 4. a) Schematic illustration of the 3D hierarchical structures. Numbers 1–3 indicated on the illustration match the corresponding features in (b). b) HR-SEM image of fluorinated hierarchical structure after thermal evaporation of the wax on a Si substrate. c) Schematic illustration of a liquid droplet on top of the re-entrant curvature formed by the hierarchical structure.

Table 1. Surface tension at 20 °C.

Liquid	σ [mN m^{-1}]
Water	72.2
Glycerol	64.5
Ethylene glycol	47.7
Benzyl chloride	38.3
Olive oil	35.1
Chlorobenzene	32
Hexadecane	27.5
Cyclohexane	25.2
Ethanol	22.4

Table 2. Contact angle hysteresis (°).

Liquid	Substrate		
	Silicon	Copper	Glass
Water	2 ± 1	2 ± 1	3 ± 1
Ethylene glycol	5 ± 1	4 ± 1	4 ± 1
Olive oil	5 ± 3	8 ± 3	14 ± 3
Hexadecane	6 ± 3	8 ± 3	15 ± 3
Ethanol	9 ± 3	7 ± 3	11 ± 3

repel the tested liquids, we measured the CAH of water, ethylene glycol, olive oil, hexadecane and ethanol on each of the substrates (**Table 2**). To examine the surface stability (the Cassie state), we performed evaporation experiments using high-purity 7 µL water droplets.

The initial measurements were intended to assess the superhydrophobic properties of the substrates. Measurement of the static contact angles for water yielded extremely high values for all examined surfaces (171°–175°), indicative of extreme hydrophobicity (**Figure 5**). The evaporation experiments demonstrated high stability of the Cassie state during droplet evaporation (which results in a change in the droplet curvature and therefore an increase in the Laplace pressure). Loss of hydrophobicity occurred only at a droplet volume of ≈0.24 µL (Figure 5).

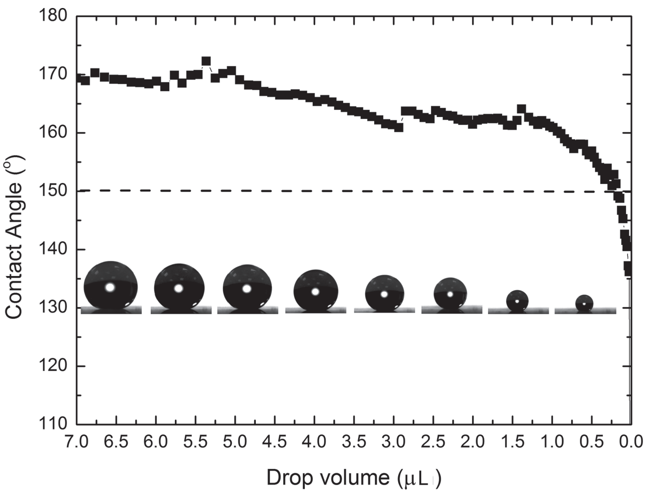

Figure 5. Contact angle as a function of droplet volume for milli-Q water on $C_{24}F_{50}$ wax evaporated on a Si substrate. Images are diminishing water droplets measured with an Attension Theta tensiometer.

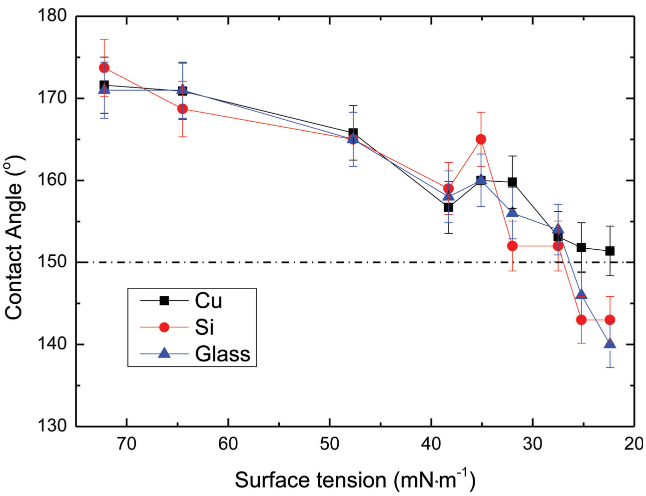

Figure 6. Contact angle as a function of surface tension on $C_{24}F_{50}$ wax evaporated on Si, Au, and Cu substrates. The tested liquids are listed in Table 1.

Static contact angle measurements obtained with various liquids are summarized in **Figure 6**. It can be seen that all surfaces maintained high contact angles (>150°) for liquids with surface tension as low as 27.5 mN m^{-1}, with the supporting Cu surface remaining superoleophobic even for liquids with surface tension as low as 22.4 mN m^{-1}. There are at least two possible explanations for this. (1) Copper surfaces exhibited the highest crystal density (3.5–5.5 µm, as seen in Figure 4a), whereas the mean distance between crystals on glass substrates varied between 4.5 and 7.5 µm. Crystal density is extremely important for the stability of a Cassie state, especially when the droplets are small and the surface tensions of the liquids are low. The effect of crystal density could be observed for low-surface-tension liquids where the penetration of liquid into the surface grooves was significant. (2) The wax crystals that formed on copper substrates exhibited a preferred orientation of (1 0 1) (Figure 1), i.e., the crystals perpendicular to the substrate were composed mostly of CF_2 groups while most of the surface crystals parallel to the substrate (i.e., the second hierarchical layer) were composed of CF_3 groups. Penetration of liquid into the surface grooves resulted in a significant increase in the contact area of liquid with the second hierarchical level of crystals. Our experimental results point to the importance of the low surface energy of the second hierarchical layer for maintaining extremely low surface tension liquids in the superoleophobic state.

The additional CAH measurements recorded in Table 2 show that these values for water and ethylene glycol on all examined surfaces were extremely low. For the Si and Cu substrates the measured CAH for all examined liquids was below 10°, indicative of the surface ability to repel the liquids by causing the droplets to roll off the surface at relatively low tilt angels. The highest CAH values were seen with glass surfaces; this can be attributed to the lower crystal density, as discussed in section 2.2.

We attribute the above results to the high surface roughness, and the re-entrant curvature, both achieved by the 3D hierarchical structure, and the choice of fluorinated wax as the surface material, resulting in a high concentration of CF_2 and CF_3 groups at the sample surface.

3. Conclusions

This report describes a novel, single-step and single-component method for the fabrication of bio-inspired hierarchical superoleophobic surfaces, by means of self-assembly of ultra-low surface energy fluorinated wax during its thermal deposition. The method can be applied to a vast variety of surfaces. The thermal deposition results in crystalline, oriented, three-dimensional hierarchical structures. These structures are characterized by marked surface roughness and re-entrant curvature which, in combination with the low surface energy of the fluorinated wax, results in high contact angles of low-surface-tension liquids and low CAH values. In addition to their superoleophobic properties, our substrates present extreme superhydrophobic qualities (CAH as low as 2° and CA >170°) with exceptional surface stability lasting over many months.

Because of the ease of its fabrication and the variety of substrates that can be used, the proposed fabrication method can be utilized for a variety of applications.

4. Experimental Section

Sample Preparation: Samples were prepared by thermal deposition of fluorinated wax on silicon, glass, gold, and copper substrates using a Moorfield MiniLab evaporator. The wax, $C_{24}F_{50}$ perfluorotetracosane, was purchased from Sigma-Aldrich (Saint-Quentin Fallavier, France). The deposition procedure was conducted in a vacuum chamber at 5×10^{-6} mbar. Samples were positioned on a holder 7–8 cm or 12–14 cm above a crucible loaded with 40–50 mg of wax. In the former case hierarchical structures were formed, however in the latter case only a single hierarchy was achieved and therefore we only relate to the former case in this paper. The system was slowly heated from 70 °C to 100 °C, and evaporation occurred at ≈100 °C during a 2-min time period. Evaporated specimens were transferred to room temperature (25 °C).

Characterization: Wax powder and crystalline thin films were characterized structurally and microstructurally by XRD with a Cu anode sealed tube (Rigaku, SmartLab, X-Ray Diffractometer). Surface imaging was performed by HR-SEM (Zeiss Ultra Plus). Micrographs were obtained at different times after deposition. Roughness and in situ time-dependent roughness were measured under confocal microscopy (Leica 3D DCM).

To characterize wettability, contact angles were measured with an Attension Theta optical tensiometer. Wettability was measured with high-purity water (milli Q), ethylene glycol (99.5%; Merck), glycerol (99.5%; JT Baker), benzyl chloride (≥99%; Merck), chlorobenzene (99%; Sigma Aldrich), hexadecane (99%; Sigma-Aldrich), ethanol (99%; Frutrom) and olive oil, each with a droplet volume of 7 µL.

For the droplet evaporation experiments 7 µL droplets of high-purity water were used.

Acknowledgements

We thank Dr. Oleg Kreinin from the Department of Materials Science & Engineering at the Technion for assembling the evaporation system and helping with the thermal deposition, and Gidon Leader from the Department of Materials Science & Engineering at the Technion for the help with the contact-angle measurements. This work was funded by the Allon Fellowship of B. Pokroy.

Received: December 30, 2012
Revised: March 11, 2013

---

[1] B. Bhushan, Y. C. Jung, *Prog. Mater. Sci.* **2011**, *56*, 1.
[2] a) J. Chapman, F. Regan, *Adv. Eng. Mater.* **2012**, *14*, B175; b) J.-S. Chung, B. G. Kim, S. Shim, S.-E. Kim, E.-H. Sohn, J. Yoon, J.-C. Lee, *J. Colloid Interface Sci.* **2012**, *366*, 64.
[3] a) B. Bhushan, K. Koch, Y. C. Jung, *Appl. Phys. Lett.* **2008**, *93*, 093101; b) B. Bhushan, K. Koch, Y. C. Jung, *Ultramicroscopy* **2009**, *109*, 1029; c) A. Nakajima, K. Hashimoto, T. Watanabe, K. Takai, G. Yamauchi, A. Fujishima, *Langmuir* **2000**, *16*, 7044.
[4] a) P. Tourkine, M. Le Merrer, D. Quéré, *Langmuir* **2009**, *25*, 7214; b) L. Mishchenko, B. Hatton, V. Bahadur, J. A. Taylor, T. Krupenkin, J. Aizenberg, *ACS Nano* **2010**, *4*, 7699; c) P. Kim, T. S. Wong, J. Alvarenga, M. J. Kreder, W. E. Adorno-Martinez, J. Aizenberg, *ACS Nano* **2012**, *6*, 6569; d) A. J. Meuler, G. H. McKinley, R. E. Cohen, *ACS Nano* **2010**, *4*, 7048.
[5] X. Gao, L. Jiang, *Nature* **2004**, *432*, 36.
[6] a) C. Neinhuis, W. Barthlott, *Ann. Bot.* **1997**, *79*, 667; b) K. Koch, B. Bhushan, W. Barthlott, *Soft Matter* **2008**, *4*, 1943; c) W. Barthlott, C. Neinhuis, *Planta* **1997**, *202*, 1.
[7] K. Koch, B. Bhushan, Y. C. Jung, W. Barthlott, *Soft Matter* **2009**, *5*, 1386.
[8] a) M. Nosonovsky, B. Bhushan, *Adv. Funct. Mater.* **2008**, *18*, 843; b) N. Michael, B. Bhushan, *Microelectron. Eng.* **2007**, *84*, 382; c) E. Bittoun, A. Marmur, *Langmuir* **2012**, *28*, 13933; d) S. Herminghaus, *EPL* **2007**, *52*, 165; e) D. Quéré, *Annu. Rev. Mater. Res.* **2008**, *38*, 71; f) M. Callies, D. Quere, *Soft Matter* **2005**, *1*, 55; g) A. Marmur, *Langmuir* **2003**, *19*, 8343.
[9] T. Young, *Philos. Trans. R. Soc.* London **1805**, *95*, 65.
[10] R. N. Wenzel, *Ind. Eng. Chem.* **1936**, *28*, 988.
[11] A. B. D. Cassie, S. Baxter, *Trans. Faraday Soc.* **1944**, *40*, 546.
[12] C. Extrand, *Langmuir* **2003**, *19*, 3793.
[13] A. K. Kota, Y. Li, J. M. Mabry, A. Tuteja, *Adv. Mater.* **2012**, *24*, 5838.
[14] K. Tsujii, T. Yamamoto, T. Onda, S. Shibuichi, *Angew. Chem. Int. Ed.* **1997**, *36*, 1011.
[15] A. Lafuma, D. Quéré, *Nat. Mater.* **2003**, *2*, 457.
[16] M. Nosonovsky, *Langmuir* **2007**, *23*, 3157.
[17] a) E. F. Hare, E. G. Shafrin, W. A. Zisman, *J. Phys. Chem.* **1954**, *58*, 236; b) T. Nishino, M. Meguro, K. Nakamae, M. Matsushita, Y. Ueda, *Langmuir* **1999**, *15*, 4321.
[18] A. Tuteja, W. Choi, M. Ma, J. M. Mabry, S. A. Mazzella, G. C. Rutledge, G. H. McKinley, R. E. Cohen, *Science* **2007**, *318*, 1618.
[19] Y. C. Jung, B. Bhushan, *Langmuir* **2009**, *25*, 14165.
[20] a) M. Nicolas, F. Guittard, S. Géribaldi, *Angew. Chem. Int. Ed.* **2006**, *45*, 2251; b) T. Darmanin, F. Guittard, S. Amigoni, E. Tafin de Givenchy, X. Noblin, R. Kofman, F. Celestini, *Soft Matter* **2011**, *7*, 1053.
[21] H. Wang, Y. Xue, T. Lin, *Soft Matter* **2011**, *7*, 8158.
[22] K. Ellinas, A. Tserepi, E. Gogolides, *Langmuir* **2011**, *27*, 3960.
[23] X. Deng, L. Mammen, H.-J. Butt, D. Vollmer, *Science* **2012**, *335*, 67.
[24] S. Pan, A. K. Kota, J. M. Mabry, A. Tuteja, *J. Am. Chem. Soc.* **2012**, *135*, 578.
[25] T. S. Wong, S. H. Kang, S. K. Y. Tang, E. J. Smythe, B. D. Hatton, A. Grinthal, J. Aizenberg, *Nature* **2011**, *477*, 443.
[26] W. Chen, A. Y. Fadeev, M. C. Hsieh, D. Öner, J. Youngblood, T. J. McCarthy, *Langmuir* **1999**, *15*, 3395.
[27] S. Pechook, B. Pokroy, *Adv. Funct. Mater.* **2012**, *22*, 745.
[28] A. Tuteja, W. Choi, G. H. McKinley, R. E. Cohen, M. F. Rubner, *MRS Bull.* **2008**, *33*, 752.